Journal of Photochemistry and Photobiology A: Chemistry 199 (2008) 34–41

Contents lists available at ScienceDirect

Journal of Photochemistry and Photobiology A: Chemistry

journal homepage: www.elsevier.com/locate/jphotochem

The family of furocoumarins: Looking for the best photosensitizer for phototherapy

Juan José Serrano-Pérez, Remedios González-Luque, Manuela Merchán, Luis Serrano-Andrés*

Instituto de Ciencia Molecular, Universitat de València, Apartado de Correos 22085, ES-46071 Valencia, Spain

ARTICLE INFO

Article history:
Received 6 February 2008
Received in revised form 25 March 2008
Accepted 18 April 2008
Available online 29 April 2008

Keywords:
Phototherapy
Furocoumarins
Triplet state
Intersystem crossing
Spin–orbit coupling

ABSTRACT

Furocoumarins are widely used as photosensitizers in photochemical therapies against different skin disorders such as psoriasis and vitiligo. Absorption of near-UV light by the chromophore triggers a set of photoreactions related to the therapeutic properties of the technique: linkage of a furocoumarin to thymine DNA nucleobases preventing proliferation of pathogenic cells, or generation of highly reactive singlet oxygen in damaged tissues. The family of furocoumarins has been studied in depth for many years seeking a drug having the most remarkable set of properties to act as a photosensitizer. For this purpose, understanding the underlying photochemical mechanisms behind the effectiveness of this therapy is required. We have undertaken a quantum-mechanical study on the photophysics and photochemistry of several relevant furocoumarins: psoralen, 8-methoxypsoralen (8-MOP) and 5-methoxypsoralen (5-MOP), 4,5′,8-trimethylpsoralen (TMP), 3-carbethoxypsoralen (3-CPS), and khellin, analyzing the most efficient way in which the lowest excited triplet state, as protagonist of the photosensitizing action, is populated from the initially promoted singlet states. The results point out to khellin, in particular, and 5-MOP, as the most efficient photosensitizers.

1. Introduction

Phototherapy, a technique consisting in the employment of electromagnetic radiation coupled with a drug, the photosensitizer, is probably the medical area which nowadays better represents the connection between Physics, Chemistry, and Medicine. The absorption of electromagnetic radiation by the chromophore triggers a chain of photochemical reactions responsible for the healing process. Phototherapy is presently considered a major therapeutic strategy for health care in dermatology and has dramatically influenced the treatment of many skin disorders, whereas its prospective application against cancer is under intense research. Not only does therapeutic photomedicine pursue the suppression of ongoing deterioration processes, but also aims to prevent, modulate or abrogate the pathogenic mechanisms causing the disease [1].

Furocomarins are well-known heterocyclic photosensitizers already used to treat some skin problems in ancient India and Egypt [2]. The treatment coined PUVA (psoralen + UV-A) therapy, in which the chromophore absorbs near UV-A light (320–400 nm, *i.e.*, 3.83–3.06 eV) [2,3–7], has been specifically designed to treat different skin disorders such as psoriasis and vitiligo [8–11]. Two are the mechanisms involving light and phototherapeutical response (see Fig. 1) [12]. On the one hand, furocoumarin in its lowest triplet excited state can undergo photoreactions with thymine forming monoadducts and diadducts inserted in the DNA strand that alter the genetic material of the affected cell, preventing its proliferation [13–16]. A [2 + 2]-photocycloaddition between the double bonds of the furocoumarin (C_3=C_4 and C_4'=C_5', see Fig. 2) and the double bond of thymine takes place [17]. On the other hand, in a second type of strategy, named photodynamic therapy (PDT), the photosensitizer in its lowest triplet excited state can transfer its excess energy to molecular oxygen available in the cellular environment, generating highly electrophilic singlet oxygen ready to damage target tissues [18–20].

In the last century, furocoumarin's chemistry reached its heyday. In 1834, Kalbruner isolated 5-methoxypsoralen (5-MOP), and Abdel Monem El Mofty made a breakthrough employing 8-methoxypsoralen (8-MOP) treating vitiligo in the 1940s. In 1953, Lerner, Denton, and Fitzpatrick, and later Parrish in 1974 [9], published studies of the treatment of both psoriasis and vitiligo with 8-MOP coupled with UV-A radiation. In the 1950s, 8-MOP was made available commercially, followed later by the synthetic compound 4,5′,8-trimethylpsoralen (TMP) [14].

Regarding the present use of furocoumarins, 8-MOP is used as an oral photoactive chemical for the treatment of vitiligo [2] and psoriasis [9]. 5-MOP is used against psoriasis as well, although it shows less severe secondary effects than 8-MOP and it is better tol-

* Corresponding author. Tel.: +34 963544427; fax: +34 963543274.
E-mail address: Luis.Serrano@uv.es (L. Serrano-Andrés).

1010-6030/$ – see front matter © 2008 Elsevier B.V. All rights reserved.
doi:10.1016/j.jphotochem.2008.04.013

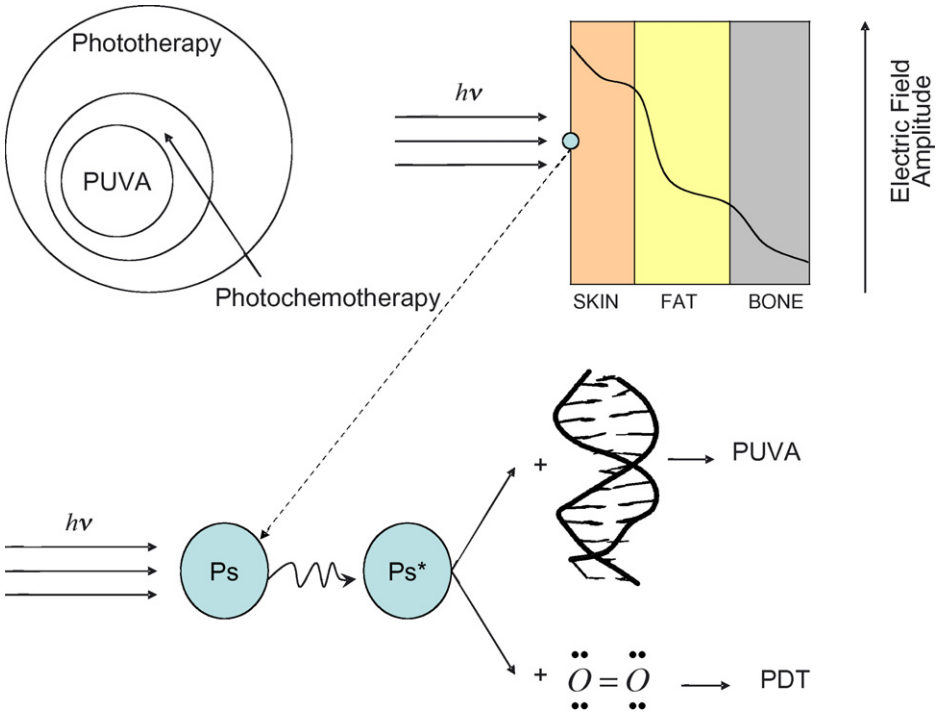

Fig. 1. Scheme of the phototherapeutical action of furocoumarins over skin diseases, including PUVA (Psoralen (Ps) + UV-A) therapy, involving formation of adducts with DNA, and PDT (photodynamic therapy), yielding reactive singlet oxygen.

erated by patients because of its lower phototoxicity [2,15]. Khellin has been found to be useful in the photochemotherapeutic treatment of vitiligo [15]. This compound does not display long-term side effects and phototoxic skin erythema reactions and seems to form mainly monoadducts. With respect to TMP, it is used in the treatment of both psoriasis and vitiligo [21]. Finally, 3-CPS (3-carbethoxypsoralen) has been tested in the photochemotherapy of psoriasis [22]. Apparently, it gives rise only to monoadducts with DNA, being considered as a non-carcinogenic alternative to 8-MOP, so it is possible that phototherapy with 8-MOP will give way to 3-CPS in a foreseeable future [23]. In summary: (i) all the mentioned furocoumarins produce monoadducts; (ii) only psoralen and TMP show a very strong ability to build diadducts; (iii) 5-MOP and 8-MOP do not have such a pronounced trend; and finally, (iv) diadducts are not obtained from 3-CPS and khellin [19,24]. Regarding the generation of singlet oxygen, psoralen (Ps), 8-MOP, and 3-CPS have been suggested as the most favorable sources [19,22,25–28].

The photochemical process leading to the therapeutic action begins with the absorption of UV-A light by the photosensitizer and the system evolution along the paths and mechanisms promoting the population of the reactive lowest energy triplet state, which must be activated only at the target tissues. From this standpoint, an effective photosensitizer should possess, in principle, certain desirable key features: it must be harmless in the dark; in order to treat deep tissues, it should be activated by long-wavelength light, because the longer wavelength radiation the photosensitizer absorbs, the deeper the energy penetrates in the tissue; its triplet state must be populated from the excited singlet state by an efficient intersystem crossing process, and effective in transferring the energy to molecular oxygen in the PDT mechanism, and finally, the chromophore should form monoadducts with DNA to become mutagenic for the cells carrying the disease and perhaps less prone to build diadducts in order to prevent carcinogenic side effects. In addition, a good photosensitizer should be amphiphilic to favor the injected administration of the drug, easily synthesized or isolated from natural sources, be deactivated soon after the treatment, and quickly eliminated from the body [29].

As a first step, and in order to understand the basic mechanistic aspects of the furocoumarins phototherapeutic action and in order to propose new and more efficient photosensitizers, it is necessary to get a better insight into the photophysics of the family of molecules. In the present research we will focus on the parent molecule, psoralen, and several of its closest derivatives: 8-MOP, 5-MOP, khellin, TMP, and 3-CPS (see Fig. 3), many of them used in current clinical practice. It would be highly desirable to have a detailed account of the photophysics of most furocoumarins to perform a thorough comparison. The experimental data are however scarce. The basic trends of the absorption spectra are in all cases similar. Apart from several sharp features at higher energies, psoralen displays a weak and structured low-lying band with a maximum ranging from 360 to 310 nm (3.44–4.00 eV) in aqueous solution and ethanol [30,31]. The intensity pattern varies for the series of furocoumarin compounds and the position of the band maximum is strongly solvent dependent: 340 nm (3.60 eV) for 8-MOP in different environments [32,33]; 335 nm (3.66 eV) in ethanol, 334–305 nm (3.71–4.02 eV) in dioxane, and 313 nm (3.91 eV) in water for 5-MOP [34,35]; 338–320 nm (3.62–3.83 eV) for khellin in various solvents [36,37]; 335 nm (3.66 eV) for TMP

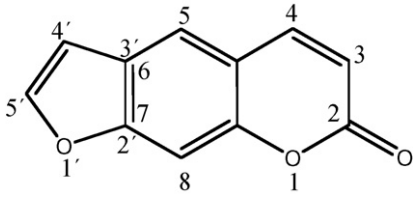

Fig. 2. Labeling and structure of psoralen.

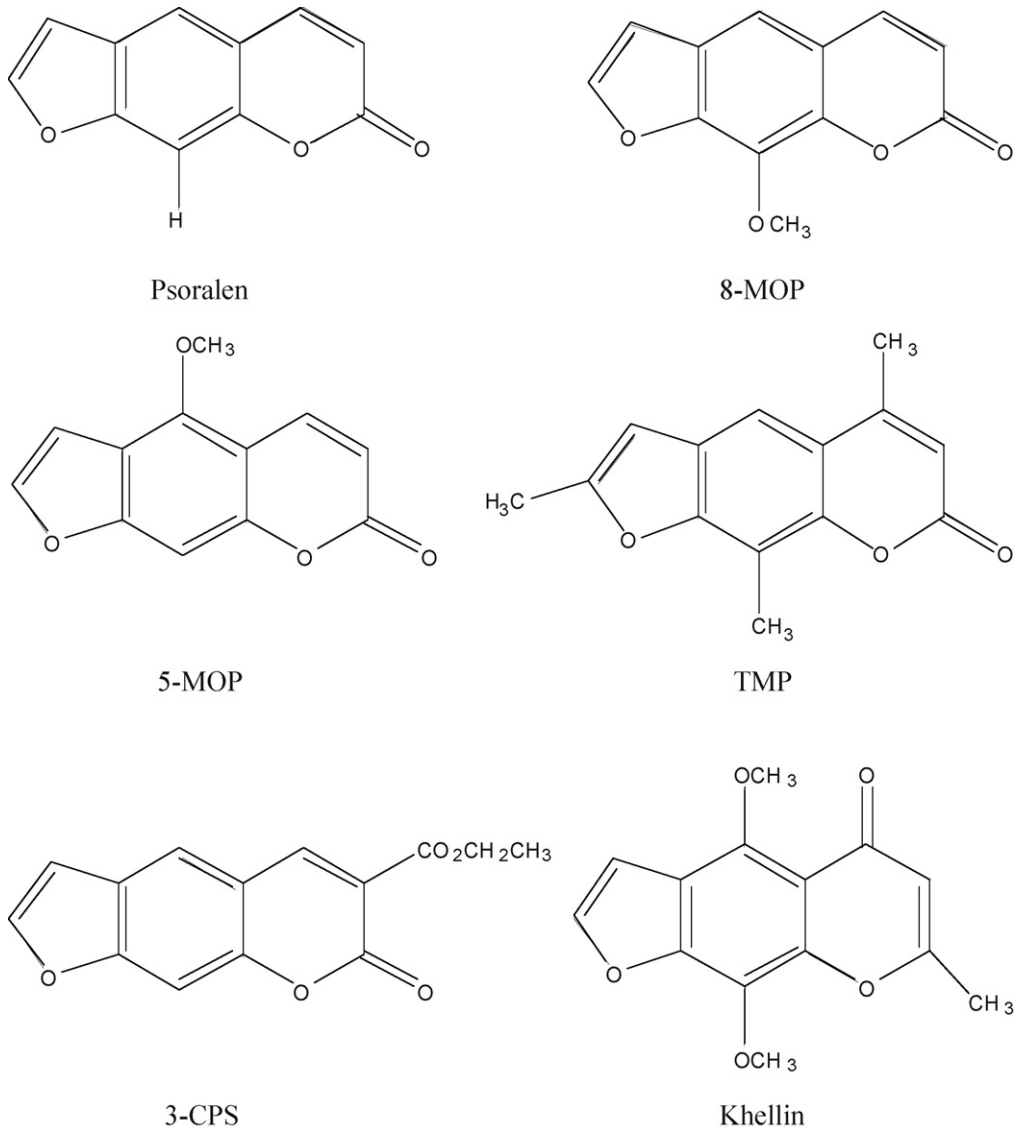

Fig. 3. Structure of psoralen, 8-MOP, 5-MOP, TMP, 3-CPS, and khellin.

in several media [21,34], and 318 nm (3.85 eV) in both water and ethanol–water mixture for 3-CPS [38]. Independently of the location of the maxima, this electronic transition is undoubtedly responsible for the UV-A absorption, source of the phototherapeutic action.

Both fluorescence (F) and phosphorescence (P) emissions have been detected for the different compounds in a similar energy range: for psoralen in ethanol at 409 nm (F, 3.03 eV) and 456 nm (P, 2.72 eV, band origin) [30]; for 8-MOP in different solvents and temperatures at 482–440 nm (F, 2.54–2.78 eV) and 456.5 nm (P, 2.68 eV, band origin) [21,34–36,39,40]; for 5-MOP at 510–425 nm (F, 2.40–2.88 eV) and 472 nm (P, 2.60 eV, band origin) in various media [21,32,34,35]; for khellin emission ranges from 553 to 422 nm (2.22–2.90 eV) [36,37]; for TMP in ethanol fluorescence has been detected from 450 to 416 nm (2.72–2.94 eV), and the phosphorescence band origin is located at 446.5 nm (2.74 eV) [34,40], and finally for 3-CPS the emission band maxima takes place at 448–395 nm (F, 2.50–2.77 eV) and 490 nm (P, 2.53 eV), depending on the temperature [23,38]. The measured fluorescence quantum yield is similar (0.02) in psoralen, 5-MOP, and 3-CPS, somewhat higher for TMP, and lower for 8-MOP and khellin [21,34,36,37]. Together with this parameter, that indicates that 8-MOP and khellin fluorescence is better quenched, we can use the phosphorescence/fluorescence quantum yield ratio (Φ_P/Φ_F) as a good probe of how favorable is the global intersystem crossing process. Comparing data in the same environment, ethanol at 77 K, the Φ_P/Φ_F ratio ranges from 7.1 in psoralen to 13.1 in 8-MOP, 11.9 in 5-MOP, and 6.0 in TMP [34], indicating that the relative population of the triplet state is the highest in 8-MOP. Khellin and 3-CPS, on the other hand, seem to give rise to higher triplet quantum yield formation than the other compounds in several solvents [22,23,36,37]. Such experimental evidence points out toward 8-MOP and khellin, and perhaps 3-CPS, as the most promising photosensitizers, considering that the efficient population of the T_1 state is a *sine qua non* condition to display an effective action via PDT and PUVA therapies [15].

The strong dependence of the data on the solvent and thermal effects and the lack of systematic and modern photochemical studies on the molecules make the rationalization of their properties quite difficult, because in many cases they cannot be compared. Apart from that, there is not a straightforward relationship between the photophysical and phototherapeutic properties, because the

latter strongly relies on the ability for subsequent formation for mono- and diadducts with DNA nucleobases. In the present study we have the objective to determine theoretically the intrinsic and most relevant photophysical properties of the furocoumarins in order to put them into the same framework and proceed to a full comparison. In particular we will analyze the efficiency of the initial population of the spectroscopic bright state, the accessibility of the singlet–triplet crossing (STC) and conical intersection (CI) regions connecting the excited states potential energy surfaces and leading to efficient intersystem crossing (ISC) and internal conversion (IC) processes, respectively, and the strength of the spin–orbit coupling terms between the different states. One of the highest level quantum-chemical methods currently available, in particular the CASPT2 approach, will be used for that purpose. The results are expected to provide good hints addressed to propose the most effective photosensitizer among the studied systems. Comparison with other quantum-chemical results on the psoralen itself can be also performed [41–43].

2. Methods and computational details

Using CASSCF multiconfigurational wave functions as reference, a second-order perturbation theory through the CASPT2 method was employed in order to include dynamic correlation energy in the calculation of the electronic excited states. The CASPT2 method calculates the first-order wave function and the energy up to second order and has repeatedly proved its accuracy [44–49]. The imaginary level-shift technique was employed in order to prevent the effect of intruder states. A shift parameter of 0.3 au was selected to avoid intruder states problems [50,51]. The molecular symmetry was constrained to the C_s point group. For geometry optimizations, however, relaxing the symmetry constraints had no effect on the final structures, which preferred in all the cases to maintain planarity. An atomic natural orbital (ANO-L)-type basis set contracted to C,O [4s3p1d]/H [2s1p] [52] was used throughout. The carbon and oxygen 1s core electrons were kept frozen in the second-order perturbation step. Geometries were obtained by computing analytical gradients at the RASSCF level for the ground and lowest singlet and triplet excited states. In the optimization of the A′ states an active space of 14 active orbitals and 16 electrons has been employed and up to quadruple excitations were considered (eight orbitals in RAS1 space and six orbitals in RAS3 space). Within the irreducible representations (a′, a″) of the C_s group this active space can be labeled as (0, 14), with no a′ and 14 a″ orbitals. An additional oxygen lone-pair orbital and two electrons were included in the active space (1, 14) in order to optimize the lowest A″ excited states. In all the remaining calculations, CASSCF wave functions were generated as state-average (SA)-CASSCF roots of a given symmetry. Using the information obtained by analyzing natural orbital occupation in control RASSCF calculations, the active space for the CASSCF calculations was set to include 12 active electrons and 12 active orbitals (0, 12) for A′ roots and 14 active electrons and 13 active orbitals (1, 12) for A″ roots. The number of selected SA-CASSCF roots was 11, 4, 7, and 3 for ^{1}A′, ^{3}A′, ^{1}A″, and ^{3}A″ symmetries, respectively. A detailed account of employed active spaces for psoralen derivatives can be found in Table 1. The CAS state interaction method [53] (CASSI) was used to compute transition properties, including the spin–orbit coupling (SOC) elements between selected states [54,55]. All calculations in the present paper were performed with the MOLCAS-6.0 quantum chemistry software [56,57].

Table 1
Active orbitals (a′, a″) and electrons (N·e$^-$) comprising the active space of the studied psoralen derivatives

	RASSCF (A′)			RASSCF (A″)			CASSCF (A′, A″)	
	RAS1	RAS3	N·e$^-$	RAS1	RAS3	N·e$^-$	RAS2	N·e$^-$
Psoralen	(0, 8)	(0, 6)	16	(1, 8)	(0, 6)	18	(1, 12)	14
8-MOP	(0, 9)	(0, 6)	18	(1, 9)	(0, 6)	20	(1, 11)	12
5-MOP	(0, 9)	(0, 6)	18	(1, 9)	(0, 6)	20	(1, 11)	12
TMP	(0, 8)	(0, 6)	16	(1, 8)	(0, 6)	18	(1, 10)	14
Khellin	(0, 10)	(0, 6)	20	(1, 10)	(0, 6)	22	(1, 9)	12
3-CPS	(0, 8)	(0, 7)	16	(1, 8)	(0, 7)	18	(1, 9)	12

3. Results and discussion

3.1. Photophysics of furocoumarins

In previous studies, the photophysics of the furocoumarin's parent molecule, psoralen, was analyzed in depth [58–60]. In particular, we computed the spectroscopic properties of the low-lying singlet and triplet excited states, as well as the basic photochemical features that makes the system an efficient photosensitizer, such it is the possibility of effectively populate its lowest energy triplet state (T_1, $\pi\pi^*$) from the initially promoted bright singlet state (S_1, $\pi\pi^*$). As mentioned above, the present paper will be devoted to make a thorough comparison of the photophysical properties of several psoralen derivatives, 8-MOP, 5-MOP, Khellin, TMP and 3-CPS, most of them used in current clinical practice, in the quest of the best photosensitizer. For that purpose we have computed vertical absorption and adiabatic excited state energies, oscillator strengths, radiative lifetimes, spin–orbit coupling terms, and relevant geometrical parameters of the two lowest energy singlet and triplet $\pi\pi^*$ and $n\pi^*$ excited states, as compiled in Tables 2 and 3.

The initially promoted S_1 $\pi\pi^*$ (S_π) state is clearly higher in energy for psoralen, 8-MOP and 5-MOP, whereas the associated transitions have not large oscillator strengths. Khellin and TMP, on the other hand, have transitions in the low near-UV range which are predicted relatively more intense, representing undoubtedly an advantage from the photochemical viewpoint. 3-CPS represents an intermediate situation. The vertical results are however difficult to relate to the variable position of the band maximum in different solvents [21–40]. The emission properties of the state are in all cases

Table 2
Main spectroscopic properties of furocoumarins[a]

Compound	S_0	S_π					S_n					T_π					T_n				
	μ (D)	E_{VA}	f	T_e	τ_{rad} (ns)	μ (D)	E_{VA}	f	T_e	τ_{rad}	μ (D)	E_{VA}	T_e	τ_{rad}	SOC	μ (D)	E_{VA}	T_e	τ_{rad} (ms)	SOC	μ (D)
Psoralen	6.25	3.98	0.027	3.59	74	6.50	5.01	$\approx10^{-4}$	3.91	3 μs	2.07	3.27	2.76	28 s	$<10^{-1}$	5.40	4.85	3.84	9	46	2.15
8-MOP	6.78	3.90	0.006	3.50	254	7.33	5.01	$\approx10^{-4}$	3.91	3 μs	2.66	3.16	2.72	60 s	$<10^{-1}$	6.75	4.85	3.84	1	47	2.77
5-MOP	7.79	3.96	0.002	3.60	971	8.15	5.05	$\approx10^{-4}$	3.95	3 μs	3.26	3.14	2.66	95 s	$<10^{-1}$	7.38	4.89	3.88	0.1	47	3.33
Khellin	4.41	3.52	0.012	3.26	189	5.15	4.00	$\approx10^{-6}$	3.26	3 ms	2.43	3.05	2.83	3.4 h	< 1	4.29	3.61	3.03	9	40	2.43
TMP	6.56	3.57	0.06	3.25	38	7.35	4.92	$\approx10^{-4}$	3.91	3 μs	1.90	3.04	2.63	180 s	$<10^{-1}$	6.13	4.78	3.73	1	46	2.06
3-CPS	4.01	3.73	0.03	3.05	100	5.31	4.84	$\approx10^{-4}$	3.59	4 μs	0.66	2.88	2.40	81 s	$<10^{-1}$	3.67	4.72	3.58	32	44	0.49

Energies in eV and SOCs between the ground and the excited state in cm^{-1}.

[a] Dipole moments (μ, D), vertical absorption (E_{VA}, eV), oscillator strength (f), adiabatic electronic band origin (T_e, eV), radiative lifetime (τ), and spin–orbit coupling (SOC, cm^{-1}).

Table 3
Selected bond lengths (P: pyrone; F: furan) at the excited states optimized geometries of furocoumarins

Compound	d (C=C)$_F$ (Å)[a]					d (C=C)$_P$ (Å)[b]				
	S_0	S_π	S_n	T_π	T_n	S_0	S_π	S_n	T_π	T_n
Psoralen	1.348	1.365	1.345	1.344 (0.05, 0.00)[c]	1.345	1.342	1.373	1.428	1.469 (0.31, 0.73)	1.419
8-MOP	1.346	1.362	1.343	1.342 (0.05, 0.00)	1.343	1.341	1.382	1.426	1.469 (0.32, 0.76)	1.417
5-MOP	1.345	1.365	1.343	1.343 (0.00, 0.04)	1.343	1.342	1.377	1.427	1.467 (0.29, 0.78)	1.420
Khellin	1.337	1.352	1.339	1.444 (0.81, 0.19)	1.339	1.332	1.328	1.351	1.333 (0.00, 0.08)	1.346
TMP	1.348	1.365	1.346	1.345 (0.06, 0.14)	1.346	1.345	1.374	1.429	1.475 (0.34, 0.66)	1.421
3-CPS	1.343	1.363	1.363	1.342 (0.00, 0.02)	1.343	1.344	1.418	1.442	1.472 (0.40, 0.71)	1.435

[a] Bond $C_{4'}C_{5'}$
[b] Bond C_3C_4 except for khellin, which is C_2C_3
[c] Spin population at the carbons located in the reactive double bonds of each moiety.

similar, whereas the computed radiative lifetimes (Strickler–Berg approach [61]) tend to be close or one order of magnitude larger than the experimental values (~1–100 ns) [35], reflecting in that manner the presence of actual non-radiative decay channels. From Table 3 it is clear that, as it was already observed in psoralen [58], the S_π state is delocalized in all the molecule, and no significant bond elongation is observed upon geometrical optimization for the representative double bonds of the furan ($C_{4'}C_{5'}$) and pyrone units (C_3C_4, except for khellin, in which it is C_2C_3). 3-CPS is, however, an exception where the C_3C_4 bond enlarges in the state, clearly because the influence of the neighbor ethylmethanoate substituent. Other singlet excited $\pi\pi^*$ states have been computed at the same level of theory for all six systems at energies 0.5–1.0 eV higher than those of the low-lying S_1 state, with transitions having noticeable oscillator strengths, although their importance in the present context is minor.

Regarding the lowest energy $n\pi^*$ states, S_n and T_n, they are in all cases related with the carbonyl oxygen lone pair, therefore centered in the pyrone ring. There are no major differences among their properties in the various molecules except for the case of khellin, where the excitation energies are near 1.0 eV lower, favored by the different position of the C=O bond in the pyrone ring. This brings changes also in the emission properties of S_n in khellin, which becomes isoenergetic with S_1 and displays a large radiative lifetime. With respect to the mechanism of triplet population, it is very important to notice that in khellin S_π and T_n become almost degenerate already at the Franck–Condon (FC) geometry. As shall be emphasized later, even when the SOC terms between both states are not very high at the ground-state geometry, (3 cm^{-1}), the combined effects of the SOC and the degeneracy will enhance the probability of efficient ISC toward T_n, followed subsequently by IC to T_1 $\pi\pi^*$ (T_π).

Finally, we can compare the results obtained for the lowest T_π state. The energy pattern is quite similar in all the studied compounds, that is, at the FC region the state is located 0.5–0.7 eV below any other excited state. Important differences can be, however, observed in khellin. This molecule locates the spin population of the T_π state in the C=C double bond of the furan ring ($C_{4'}C_{5'}$), unlike the other derivatives that do it on the pyrone C=C bond (C_3C_4), as it is clear by checking in Table 3 the enlargement of the corresponding bonds upon optimization of the state. A spin population concentrated at the carbon atoms of the furan double bond in the T_π state of khellin, unlike at the pyrone double bond in the other derivatives, also reflects the different behavior of the former. These facts may have dramatic consequences in the photochemistry of khellin as compared with the other systems when monoadducts are formed with thymine in the DNA strand. Whereas a T_π populated psoralen or other derivatives will favor a [2 + 2]-photocycloaddition linking an elongated pyrone (C_3C_4) bond and the double bond of thymine leading to pyrone-type monoadducts (PMA), khellin will tend to link through the double bond of the furan side, leading to furan-type monoadducts (FMA) [60]. Regarding emission properties, the obtained electronic band origins of phosphorescence are strikingly close (less than 0.1 eV) to the experimental values of vibrational band origin: psoralen (2.7 eV), 8-MOP (2.68 eV), 5-MOP (2.60 eV), and TMP (2.74 eV) [32]. On the other hand, computed phosphorescence radiative lifetimes are just one order of magnitude off from the experimental values (~1 s) [35], except for khellin, in which we obtain a value of 3.4 h (12,240 s). This result might reflect that the Strickler–Berg approach cannot be applied in the case of khellin due perhaps to the presence of non-radiative decay channels toward other states, as it will be shown in the next section. Anyway, from the viewpoint of a photosensitizer and provided that radiationless processes from T_π do not become predominant, khellin will be undoubtedly a convenient system displaying a very long-lived triplet state. More studies on its phosphorescence are surely required.

In summary, the study of the photophysics of psoralen derivatives indicates that although large differences are not expected from the parent molecule, the analyzed derivatives will be slightly more efficient sources of triplet-activated phototherapy than psoralen itself, either because the initial S_1 state is more easily populated (lower energies and larger intensities), like for khellin, TMP or 3-CPS, or because the T_π state is slightly longer lived. Khellin represents a unique situation, because the distinct pyrone ring π structure largely modifies the photophysical properties, decreasing the excitation energies and enlarging the state lifetimes, and more specifically making S_π and T_n degenerate at the FC geometry and prone to give very efficient ISC rates. The consequences for the photochemistry of the systems are also crucial. Khellin is expected to form preferably triplet (T_π)-mediated FMA complexes, because of the location of the spin population of T_π in the furan double C=C bond, unlike the other systems that will initially form pyrone monoadducts (PMA). In the next section we shall provide a deeper analysis on the mechanism of efficient population of T_π, following the scheme recently proposed for psoralen [59].

3.2. Triplet population mechanism in furocoumarins

The main goal of the present research is to determine a mechanism to efficiently populate the lowest excited triplet state in furocoumarins, given that this state is the protagonist of the photosensitizing action. In order to make fully comparable the results obtained for the psoralen derivatives with those of the parent molecule, the same methodology as in Ps has been applied [59,60]. The bright spectroscopic S_π singlet state in furocoumarins is the only one to be significantly populated by direct absorption in the range of UV-A radiation typically used in phototherapy (3.1–3.9 eV) [13–15]. Therefore, from this state we focus on how the most favorable transfer of energy to the triplet manifold can take place.

An effective ISC process demands two conditions: small singlet–triplet (S–T) energy gaps and large SOC between the populated state (S_π here) and the corresponding triplet state. According to the qualitative El-Sayed rules [62,63] the spin–orbit coupling is large between states of $\pi\pi^*$ and $n\pi^*$ types and small between states of the same character. Therefore, a large SOC matrix element between S_π (the lowest excited singlet state of $\pi\pi^*$ nature) and T_n state (the lowest excited triplet state of $n\pi^*$ nature) is likely to occur. At the ground-state FC geometry, the computed data are: Ps ($\Delta E = 0.87$ eV; SOC = 3 cm^{-1}), 8-MOP ($\Delta E = 0.95$ eV; SOC = 3 cm^{-1}), 5-MOP ($\Delta E = 0.93$ eV; SOC = 3 cm^{-1}), khellin ($\Delta E = 0.09$ eV; SOC = 3 cm^{-1}), TMP ($\Delta E = 1.21$ eV; SOC = 6 cm^{-1}), and 3-CPS ($\Delta E = 0.98$ eV; SOC = 4 cm^{-1}). The two mentioned conditions do not seem to be simultaneously fulfilled. Khellin, in which the gap S_π–T_n is 0.09 eV, whereas the SOC, even if small, 3 cm^{-1}, it is noticeable, is an exception, and, consequently the ISC process can be considered more favorable. Furthermore, taking into account the values for the dipole moments displayed in Table 2, it is not expected that the effect of the aqueous environment largely changes the outcome. In the remaining compounds an immediate ISC upon absorption is unlikely, especially because of the large energy gap and the effects of the environment. Considering the obtained relative dipole moments, the S_π and T_n states will slightly stabilize and destabilize in polar solvents, respectively, increasing the S–T gap. In any case, the molecule can evolve rapidly along the S_π hypersurface, and therefore it is possible to search for regions of the coordinate space in which both energy gap and SOC are more favorable for ISC. Provided that those regions are easily accessible they can be the sources of triplet population. The strategy we have followed in the study is the same as the one we have recently employed for psoralen [59,60]. We found that the S_π state minimum was easily reached from the FC geometry, therefore we have to be able to find crossing regions starting from such structure. As in psoralen we have performed linear interpolations in internal coordinates (LIIC) from the minimum of the S_π state to the minimum of the S_n state in each furocoumarin (see Figs. 4 and 5), to help us to understand the profiles of the different excited states along such a path, considered to be appropriate to find the singlet–triplet crossing, since both S_n and T_n states share the same basic structure and energetics [59].

Along the LIIC profile the main geometrical arrangement from the first ($0 \equiv S_\pi$ minimum) to the last ($4 \equiv S_n$ minimum) point is, as expected, an enlargement of the C=O bond, due to the change in nature from a $\pi\pi^*$ to a $n_O\pi^*$ state. Once the S_π state is populated its minimum can be easily reached, and then fluorescence is favored. Deactivation to other states by means of efficient ISC would be only possible if, simultaneously, the energy gap S–T is small enough and the SOC terms are large enough. Starting by the results on Fig. 4, in psoralen, 8-MOP, and 5-MOP the obtained profiles for the different states are apparently similar. As it occurs at the FC geometry, in the S_π minimum the two criteria for efficient ISC are not fulfilled at the same time. The SOC terms between S_π and any other excited triplet $\pi\pi^*$ state (such as T_2, T_3 or T_4) are too small, whereas they increase for the coupling between S_π and T_n (3–5 cm^{-1}). The energy gap S_π–T_n is, however, too large to expect an efficient ISC at the S_π-equilibrium structure, $(S_\pi)_{MIN}$. Studying the evolution along the LIIC path may provide valuable information on the fate of the energy. In all systems, the only state that strongly interacts with S_π via spin–orbit terms is the T_n state. Analysis of the accessibility of the STC $(S_\pi/T_n)_X$ gives a good account of the relative efficiency of the corresponding ISC process. In the three molecules the singlet–triplet crossing takes place between points 2 and 3. The approximate barriers that the system has to overcome to reach the T_n state from the S_π minimum are 0.42 eV

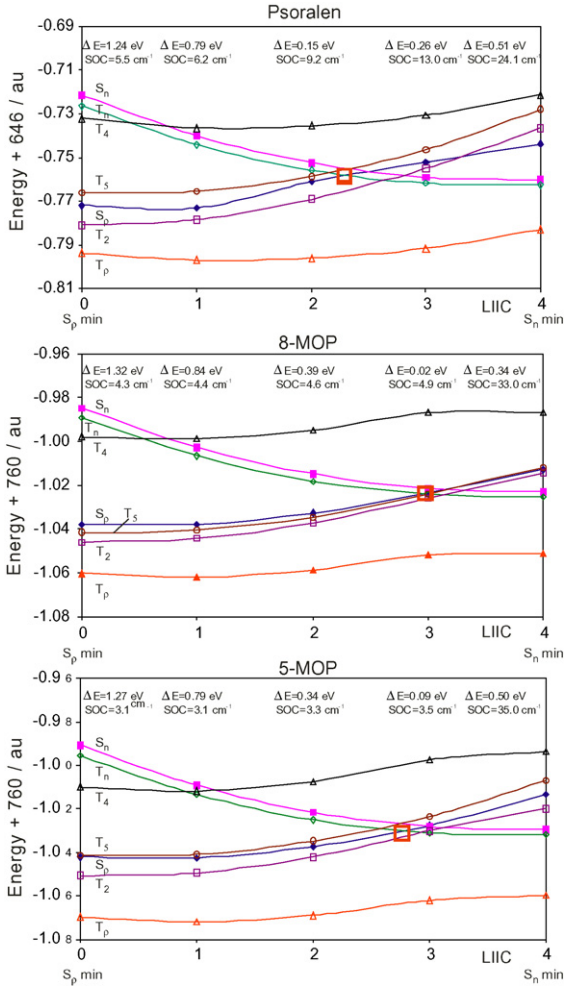

Fig. 4. Computed CASPT2 energies for the low-lying excited states of psoralen, 8-MOP, and 5-MOP along a linear interpolation of internal coordinates (LIIC) from S_π to S_n minima. Solid and dashed lines represent singlet and triplet states, respectively. Energy gaps (ΔE) and spin–orbit coupling (SOC) terms between the S_π and T_n states at each geometry are also included. The singlet–triplet crossing $(S_\pi/T_n)_X$ is indicated.

(Ps), 0.39 eV (8-MOP), and 0.26 eV (5-MOP). Because of the nature of the interpolation in the considered LIIC path, the obtained barrier can be considered as an upper limit to the actual value. In a previous study on Ps, the STC $(S_\pi/T_n)_X$ was located and the barrier decreased to 0.36 eV, that is, just 0.06 eV [59,60]. The trend is clear, and the lower barrier obtained in 5-MOP makes it be viewed as a slightly better candidate to yield more efficient ISC than psoralen and 8-MOP. It is worth noting, however, that along the LIIC path the three systems display increasing SOC elements, that become maximum at the S_n minimum, and therefore the region for significant ISC can extend from the mentioned STC to the $(S_n)_{MIN}$ structure. No drastic differences are then expected in the photophysics of the three systems.

From the results obtained for khellin, TMP, and 3-CPS displayed in Fig. 5, it is clear that TMP and 3-CPS have similar features as the previous systems, in particular a large S_π–T_n gap at the S_π minimum. As a consequence, the STC $(S_\pi/T_n)_X$ takes place far away along the LIIC profile and the corresponding barrier to reach STC $(S_\pi/T_n)_X$ from the S_π minimum is as large as in psoralen: 0.41 eV (TMP) and 0.44 eV (3-CPS). Because of such relatively higher barrier height, even when the SOC terms are slightly larger than in psoralen, 8-MOP, and 5-MOP, the efficiency of the ISC process will be probably lower. Khellin is obviously a totally different case. The S_π and T_n

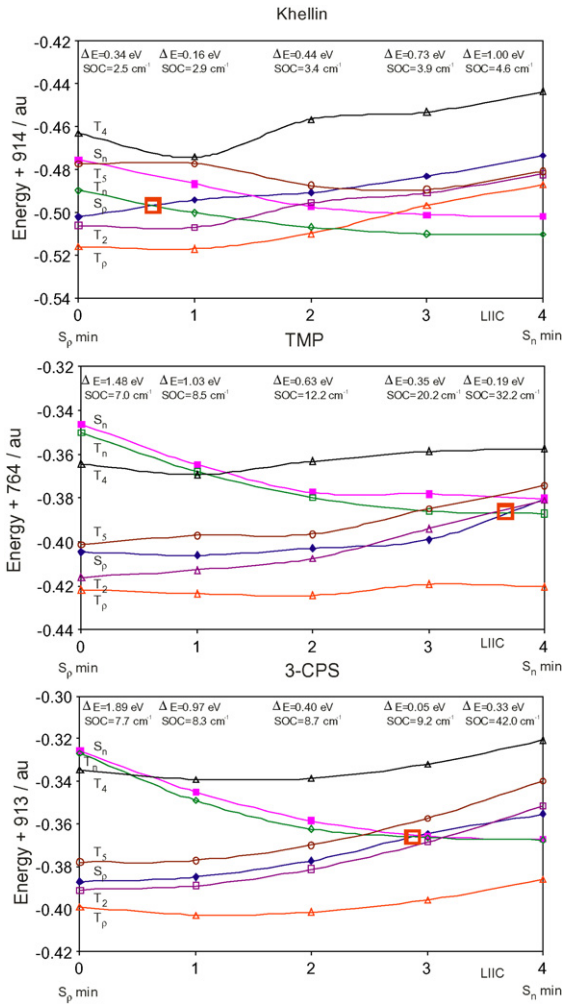

Fig. 5. Computed CASPT2 energies for the low-lying excited states of khellin, TMP, and 3-CPS along a linear interpolation of internal coordinates (LIIC) from S_π to S_n minima. Solid and dashed lines represent singlet and triplet states, respectively. Energy gaps (ΔE) and spin–orbit coupling (SOC) terms between the S_π and T_n states at each geometry are also included. The singlet–triplet crossing $(S_\pi/T_n)_X$ is indicated.

states are basically degenerated already at the FC geometry, and they are very near at the S_π minimum. The STC $(S_\pi/T_n)_X$ takes place immediately along the LIIC path. Because both states are extremely close in a wide region of the coordinate space, the computed barrier, 0.11 eV, cannot be most probably be considered as a measure of the actual efficiency of the ISC process. The energy degeneracy, together with the computed SOC coupling near 3 cm^{-1}, makes the ISC process involving S_π to T_n extremely favorable in relation to the other furocoumarins.

Once the energy has been partially transferred from S_π to the T_n state, the lower T_π state can be efficiently populated by means of a proper IC process. Fig. 6 displays a scheme of the mechanism of triplet population in furocoumarins suggested by the present results. In our previous study on psoralen [59,60], the conical intersection $(T_n/T_\pi)_{CI}$, responsible for the IC process, was located almost isoenergetic to the T_n minimum, and therefore the corresponding radiationless decay was predicted to be extremely efficient. In all the molecules studied here, except khellin, the profile of these two triplet states is very similar, and therefore the final outcome once T_n has been populated can be considered to be practically the same. Once again khellin is an exception. The T_n state is much lower in energy, and therefore the conical intersection $(T_n/T_\pi)_{CI}$ can be

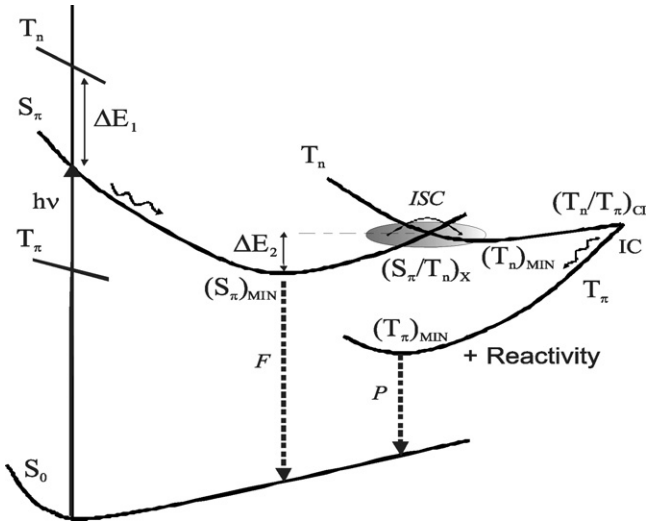

Fig. 6. Scheme of the suggested mechanism of triplet state population in furocoumarins. See text.

reached in a barrierless way already along the LIIC path, enhancing in this way the efficiency of the IC process.

In summary, we are proposing a common mechanism for the population of the lowest energy triplet state in furocoumarins which may slightly vary depending on different factors. If the FC gap between the initially populated S_π state and the T_n state (ΔE_1 in Fig. 6) is small enough, like in khellin, a very efficient ISC process will take place already near the initial FC geometry, provided that the SOC terms are large enough. In the other furocoumarins, reaching a region of favorable S_π/T_n ISC means to surmount a barrier (ΔE_2 in Fig. 6) toward the singlet–triplet crossing point. The barrier has been computed much larger in psoralen, 8-MOP, TMP, and 3-CPS than in 5-MOP, in which the ISC process can be therefore considered slightly more efficient. In all cases, but especially in khellin, once the T_n state is populated the energy transfer to the T_π state will be extremely favorable.

A photosensitizer is expected to be more effective as more efficient is the process of population of T_π, since such state is protagonist of processes as the cycloaddition to the DNA thymine moieties and the formation of singlet molecular oxygen for photodynamic therapy. From the photophysical viewpoint we have found in the studied psoralen derivatives that khellin could be considered a much more effective photosensitizer, followed by 5-MOP, whereas 8-MOP, TMP, 3-CPS, and psoralen itself, are expected to be somewhat less efficient, a tendency similar to that observed in the clinical practice [2,9,15,21,22]. In khellin, however, the triplet state reactivity is centered in the side of the furan ring, which indicates a favorable formation of furan-monoadducts (FMA), whereas the other systems have a reactive bond in the triplet state located at the pyrone ring, favoring the formation of PMA. Further research is required to determine whether the phototherapeutic efficiency of furocoumarins is better influenced by a more favorable triplet population, such as in khellin, or by the initial formation of FMA (khellin) or PMA (the other systems) complexes with DNA. Work on the formation of monoadducts furocoumarins–thymine at this level of theory is currently in process.

4. Summary and conclusions

In the present contribution, the photophysics of several furocoumarins has been analyzed using quantum-chemical methods through the multiconfigurational second-order perturbation pro-

cedure, CASPT2, employing high-quality ANO-type one-electron basis sets. Optimized geometries for the low-lying singlet and triplet states, energy differences, and state and transition properties provide relevant information to understand the excited state structure and the absorption and emission processes taking place upon irradiation of the furocoumarin class of molecules. The absorption and emission spectra of the systems have been studied by computing vertical and adiabatic excitation energies. Analysis of the energy gaps and spin–orbit couplings at the Franck–Condon region suggests that the process responsible for the population of T_1 (T_π) does not take place vertically, except in khellin, and most probably it occurs along the relaxation path on the S_1 (S_π) hypersurface. On the contrary, in khellin population of T_π is likely to happen at the Franck–Condon region. Another important difference regarding khellin is that the spin population in the T_π state is mainly located on the carbon atoms of the C=C double bond of the furan moiety, just the opposite that in psoralen, 8-MOP, 5-MOP, TMP, and 3-CPS. As a result, the length of C=C double bond of furan moiety is enlarged with respect to the ground state in the T_π state of khellin.

In addition, we have analyzed the population mechanism of the low-lying T_π state of the furocoumarins, protagonist of their action as photosensitizers. Determination of the obtained energy differences, barrier heights, energy minima, and spin–orbit coupling terms among the different electronic states indicates that the system, after evolving toward the S_π energy minimum, may surmount a barrier and reach a S–T crossing between S_π and the low-lying triplet $n\pi^*$ state, $(S_\pi/T_n)_X$. In this regard, khellin and 5-MOP, having the smallest barriers, seem to be the most promising photosensitizers. Once the T_n state has been populated, an ultrafast decay towards the low-lying T_π state may well proceed through the conical intersection $(T_n/T_\pi)_{CI}$, transferring the energy to the T_π energy minimum from which the furocoumarin molecule may emit (phosphorescence), react with thymine, or transfer its energy to molecular oxygen. Among the other molecules, khellin combines favorably the presence of an easily accessible CI with a large lifetime for the reactive T_π excited state. Considering that psoralen, 8-MOP, and 3-CPS have been estimated as the best singlet oxygen generators [19,22,25–28] and until more information is available we here suggest that khellin seems to be the most plausible photosensitizer at least on the basis to its ability to react with thymine.

Acknowledgments

The research has been supported by projects CTQ2004-01739, CTQ2007-61260, and CSD2007-0010 Consolider-Ingenio in Molecular Nanoscience of the Spanish MEC/FEDER and GV-AINF2007/051 of the *Generalitat Valenciana*. JJSP acknowledges a Ph.D. (FPU) grant from the Spanish MEC.

References

[1] M. Weichenthal, T. Schwarz, Photodermatol. Photoimmunol. Photomed. 21 (2005) 260.
[2] M.A. Pathak, T.B. Fitzpatrick, J. Photochem. Photobiol. B: Biol. 14 (1992) 3.
[3] W.L. Fowlks, J. Invest. Dermatol. 32 (1959) 249.
[4] M.A. Pathak, J.H. Fellman, Nature (London) 185 (1960) 382.
[5] J.E. Hearst, Chem. Res. Toxicol. 2 (1989) 69.
[6] N. Kitamura, S. Kohtani, R. Nagakaki, J. Photochem. Photobiol. C: Photochem. Rev. 6 (2005) 168.
[7] B.J. Parsons, Photochem. Photobiol. 32 (1980) 813.
[8] A.B. Lerner, C.R. Denton, T.B. Fitzpatrick, J. Invest. Dermatol. 20 (1953) 299.
[9] J.A. Parrish, T.B. Fitzpatrick, L. Tannembaum, M.A. Pathak, N. Eng. J. Med. 291 (1974) 1207.
[10] H. Van Weelden, E. Young, J.C. Van der Leun, Br. J. Dermatol. 103 (1980) 1.
[11] W.L. Morison, Photodermatol. Photoimmunol. Photomed. 20 (2004) 315.
[12] F. DalliÏAcqua, P. Martelli, J. Photochem. Photobiol. B: Biol. 8 (1991) 235.
[13] P.S. Song, K.J. Tapley Jr., Photochem. Photobiol. 29 (1979) 1176.
[14] E. Ben-Hur, P.S. Song, Adv. Radiat. Biol. 11 (1984) 131.
[15] D. Averbeck, Photochem. Photobiol. 50 (1989) 859.
[16] J. Cadet, P. Vigny, in: H. Morrison (Ed.), Bioorganic Photochemistry 1, John Wiley & Sons, New Jersey, 1990.
[17] F. Bernardi, M. Olivucci, M.A. Robb, Acc. Chem. Res. 23 (1990) 405.
[18] A.M. Rouhi, Chem. Eng. News 76 (1998) 22.
[19] P.C. Joshi, M.A. Pathak, Biochem. Biphys. Res. Commun. 112 (1983) 638.
[20] Y.N. Donan, R. Gurny, E. Alléman, J. Photochem. Photobiol. B: Biol. 66 (2001) 89.
[21] H. Matsumoto, A. Isobe, Chem. Pharm. Bull. 29 (1981) 603.
[22] J.C. Ronfard-Haret, D. Averbeck, R.V. Bensasson, E. Bisagni, E.J. Land, Photochem. Photobiol. 35 (1982) 479.
[23] M. Craw, R.V. Bensasson, J.C. Ronfard-Haret, M.T.S.E. Melo, T.G. Truscott, Photochem. Photobiol. 37 (1983) 611.
[24] P.C. Joshi, M.A. Pathak, Indian J. Biochem. Biophys. 32 (1995) 63.
[25] N.J. De Mol, G.M.J. Beijersbeergen van Henegouwen, Photochem. Photobiol. 33 (1981) 815.
[26] R. Bevilacqua, F. Bordin, Photochem. Photobiol. 17 (1973) 191.
[27] W. Poppe, L.I. Grossweiner, Photochem. Photobiol. 22 (1975) 217.
[28] C.N. Knox, E.J. Land, T.G. Truscott, Photochem. Photobiol. 43 (1986) 359.
[29] R. Bonnett, Chemical Aspects of Photodynamic Therapy, Gordon and Breach Science, Amsterdam, 2000.
[30] P.S. Song, S.C. Shim, W.W. Mantulin, Bull. Chem. Soc. Jpn. 54 (1981) 315.
[31] M. Collet, M. Hoebeke, J. Piette, A. Jakobs, L. Lindqvist, A. Van de Vorst, J. Photochem. Photobiol. B: Biol. 35 (1996) 221.
[32] H. Matsumoto, Y. Ohkura, Chem. Pharm. Bull. 11 (1978) 3433.
[33] D.J. Yoo, H.D. Park, A.R. Kim, Y.S. Rho, S.C. Shim, Bull. Korean Chem. Soc. 23 (2002) 1315.
[34] W.W. Mantulin, P.S. Song, J. Am. Chem. Soc. 95 (1973) 5122.
[35] T.S.E. Melo, A. Maçanita, M. Prieto, M. Bazin, J.C. Ronfard-Haret, R. Santus, Photochem. Photobiol. 48 (1988) 429.
[36] H.K. Kang, E.J. Shin, S.C. Shim, Bull. Korean Chem. Soc. 12 (1991) 554.
[37] M.L. Borges, L. Latterini, F. Elisei, P.F. Silva, R. Borges, R.S. Becker, A.L. Maçanita, Photochem. Photobiol. 67 (1998) 184.
[38] P. Vigny, F. Gaboriau, M. Duquesne, E. Bisagni, D. Averbeck, Photochem. Photobiol. 30 (1979) 557.
[39] J.H. Kim, S.W. Oh, Y.S. Lee, S.C. Shim, Bull. Korean Chem. Soc. 8 (1987) 298.
[40] T. Lai, B.T. Lim, E.C. Lim, J. Am. Chem. Soc. 104 (1982) 7631.
[41] J. Tatchen, M. Kleinschmidt, C.M. Marian, J. Photochem. Photobiol. A: Chem. 167 (2004) 201.
[42] J. Tatchen, C.M. Marian, Phys. Chem. Chem. Phys. 8 (2006) 2133.
[43] J. Tatchen, N. Gilka, C.M. Marian, Phys. Chem. Chem. Phys. 9 (2007) 5209.
[44] K. Andersson, P.-Å. Malmqvist, B.O. Roos, J. Chem. Phys. 96 (1992) 1218.
[45] L. Serrano-Andrés, M. Merchán, I. Nebot-Gil, R. Lindh, B.O. Roos, J. Chem. Phys. 98 (1993) 3151.
[46] B.O. Roos, K. Andersson, M.P. Fülscher, P.-Å. Malmqvist, L. Serrano-Andrés, K. Pierloot, M. Merchán, Adv. Chem. Phys. 93 (1996) 219.
[47] L. Serrano-Andrés, M.P. Fülscher, B.O. Roos, M. Merchán, J. Phys. Chem. 100 (1996) 6484.
[48] L. Serrano-Andrés, M. Merchán, A.C. Borin, Proc. Natl. Acad. Sci. U.S.A. 103 (2006) 8691.
[49] L. Serrano-Andrés, M. Merchán, A.C. Borin, Chem. Eur. J. 12 (2006) 6559.
[50] N. Forsberg, P.-Å. Malmqvist, Chem. Phys. Lett. 274 (1997) 196.
[51] A.C. Borin, L. Serrano-Andrés, Chem. Phys. 262 (2000) 253.
[52] P.O. Widmark, P.Å. Malmqvist, B.O. Roos, Theor. Chim. Acta 77 (1990) 291.
[53] P.Å. Malmqvist, B.O. Roos, Chem. Phys. Lett. 155 (1989) 189.
[54] M. Merchán, L. Serrano-Andrés, M.A. Robb, L. Blancafort, J. Am. Chem. Soc. 127 (2004) 1820.
[55] B.O. Roos, P.-Å. Malmqvist, Chem. Phys. Phys. Chem. 6 (2004) 2919.
[56] K. Andersson et al., MOLCAS, Version 6.0, Department of Theoretical Chemistry, Chemical Center, University of Lund, P.O.B. 124, S-221 00 Lund, Sweden 2004.
[57] V. Veryazov, P.O. Widmark, L. Serrano-Andrés, R. Lindh, B.O. Roos, Int. J. Quantum Chem. 100 (2004) 626.
[58] J.J. Serrano-Pérez, L. Serrano-Andrés, M. Merchán, J. Chem. Phys. 124 (2006) 1.
[59] J.J. Serrano-Pérez, M. Merchán, L. Serrano-Andrés, Chem. Phys. Lett. 434 (2007) 107.
[60] J.J. Serrano-Pérez, M. Merchán, L. Serrano-Andrés, Chem. Phys. 347 (2008) 422.
[61] O. Rubio-Pons, L. Serrano-Andrés, M. Merchán, J. Phys. Chem. A 105 (2001) 9664.
[62] M.A. El-Sayed, J. Chem. Phys. 38 (1963) 2834.
[63] P. Avouris, W.M. Gelbart, M.A. El-Sayed, Chem. Rev. 77 (1977) 793.